J. Cent. South Univ. (2015) 22: 1510−1520
DOI: 10.1007/s11771-015-2668-6

Springer

Impact coefficient and reliability of mid-span continuous beam bridge under action of extra heavy vehicle with low speed

LIU Bo(刘波)[1, 2], WANG You-zhi(王有志)[1], HU Peng(胡朋)[3], YUAN Quan(袁泉)[1]

1. School of Civil Engineering, Shandong University, Ji'nan 250061, China;
2. Jinan Survey and Design Branch of China Railway Tenth Group, Ji'nan 250101, China;
3. School of Civil Engineering, Shandong Jiaotong University, Ji'nan 250023, China

Abstract: To analyze the dynamic response and reliability of a continuous beam bridge under the action of an extra heavy vehicle, a vehicle–bridge coupled vibration model was established based on the virtual work principle and vehicle–bridge displacement compatibility equation, which can accurately simulate the dynamic characteristics of the vehicle and bridge. Results show that deck roughness has an important function in the effect of the vehicle on the bridge. When an extra heavy vehicle passes through the continuous beam bridge at a low speed of 5 km/h, the impact coefficient reaches a high value, which should not be disregarded in bridge safety assessments. Considering that no specific law exists between the impact coefficient and vehicle speed, vehicle speed should not be unduly limited and deck roughness repairing should be paid considerable attention. Deck roughness has a significant influence on the reliability index, which decreases as deck roughness increases. For the continuous beam bridge in this work, the reliability index of each control section is greater than the minimum reliability index. No reinforcement measures are required for over-sized transport.

Key words: continuous beam bridge; extra heavy vehicle; coupled vibration; impact coefficient; reliability

1 Introduction

Extra heavy highway transportation has become increasingly common since China joined the World Trade Organization, and the weight of heavy industrial equipments (such as stator generators, transformers, and reactors) constantly refreshes the record. The onerous tasks of accommodating over-sized transport pose challenges on the bearing capacity and reliability assessment of highway bridges. Current studies are mainly focused on bearing capacity evaluation and temporary reinforcement measures [1−3] when extra heavy vehicles cross bridges. A minimal attention has been paid to extra heavy vehicle–bridge coupled vibration and reliability assessment.

Bridges normally require temporary reinforcement when extra heavy vehicles pass through them. Only a few large-span bridges on transport routes have been established based on economic considerations. Small- and medium-span bridges account for the vast majority. Usually, traffic must be temporarily interrupted when an extra heavy vehicle crosses a bridge. Moreover, the vehicle must drive at a low speed to reduce the dynamic responses of the bridge. However, the vehicle–bridge coupled system characterized by "heavy vehicle and light bridge" and "long vehicle and short bridge" has its own unique dynamic characteristics. Requiring the vehicle to drive at a low speed is often unrealistic, and in many cases, unnecessary.

In this work, the vehicle–bridge coupled system is decomposed into two separate motion systems, namely, bridge vibration and vehicle vibration subsystems, based on the analysis of the vehicle–bridge coupled system. The displacement compatibility equation is utilized to consider the contact between the wheels and the deck [4]. A vehicle–bridge coupled vibration analysis program is developed to analyze the dynamic responses and reliability of the bridge under the action of extra heavy vehicles, with a continuous beam bridge as an example.

2 Vehicle–bridge coupled vibration model

The classical theories of vehicle–bridge dynamic interaction include the model of constant force moving at constant speed, the model of harmonic force moving at

Foundation item: Project(50779032) supported by the National Natural Science Foundation of China; Project(20090451330) supported by the Postdoctoral Foundation of China; Project(BS2013SF007) supported by Shandong Scientific Research Award Foundation for Outstanding Young Scientists, China
Received date: 2014−03−31; **Accepted date:** 2014−06−15
Corresponding author: WANG You-zhi, Professor; Tel: +86−13953176366; E-mail: wangyouzhi@sdu.edu.cn

constant speed, the model of mass rolling at constant speed, and the model of spring-mass moving at constant speed. In these models, modal superposition method and modal orthogonality are employed to deduce the dynamic balance equation of a vehicle–bridge system based on the forced vibration differential equation for a simply supported beam. A vehicle is composed of a rigid chassis (body), wheels and tires, and a variety of linear and nonlinear suspension devices. Vehicle models can be classified into three types, namely, integral vehicle model, 1/2 vehicle model, and 1/4 vehicle model, depending on the research purposes. According to the plane characteristics of the problem in this work, a 1/2 vehicle model was established to simulate an extra heavy vehicle with the same total mass, centroid location, and rotary inertia. The suspension devices and tires were modeled as a linear spring and damper. The DOFs of the rigid body, such as the ups and downs, and the pitch, were considered in the model. The generalized principle of virtual work and finite element method were utilized to derive the vibration equations of the vehicle and bridge subsystems. The displacement compatibility equation was then utilized to achieve the solution and analyze the vehicle–bridge vertical coupled vibration [5].

2.1 Vehicle model

The mass of absorption tower of Turkmenistan Chemical Plant manufactured by Weihai Chemical Machinery Factory is 488.1 t, and the total mass of the loaded flat-bed trailer is 600.6 t. The transport motorcade includes a four-axis tractor, a 25-axis flat-bed trailer, and a three-axis moped as shown in Fig. 1. Towed connection devices were utilized between vehicles that bear longitudinal loads. Given that the main concern is the vertical vibration of the vehicle–bridge system, the tractor, flat-bed trailer, and moped were considered separately.

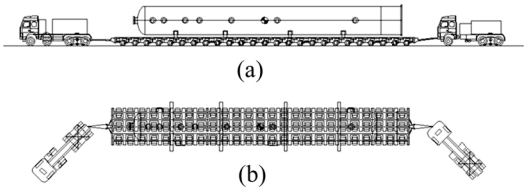

Fig. 1 Extra heavy vehicle: (a) Elevation; (b) Plan

The simplified two-series spring–mass–damper 1/2 vehicle model is shown in Fig. 2, including the four-axis tractor with four endpoints and six DOFs, the 25-axis flat-bed trailer with 25 endpoints and 27 DOFs, and the three-axis moped with three endpoints and five DOFs. The two DOFs of the vehicle bodies are vertical displacement Z_0 and rotary angle θ around the Y-axis (Fig. 2). M denotes the body mass; m_i is the sum of the wheel and suspension device with each block mass corresponding to a vertical displacement freedom Z_i; K_{di} and C_{di} are the vertical stiffness and damping of series one, respectively; and K_{ui} and C_{ui} denote the vertical stiffness and damping of series two, respectively. i=1, 2,⋯, N. N=4, N=25, and N=3 for the tractor, flat-bed trailer, and moped, respectively. L, L_1−L_4 denote the longitudinal distance between the axles and the centroid respectively.

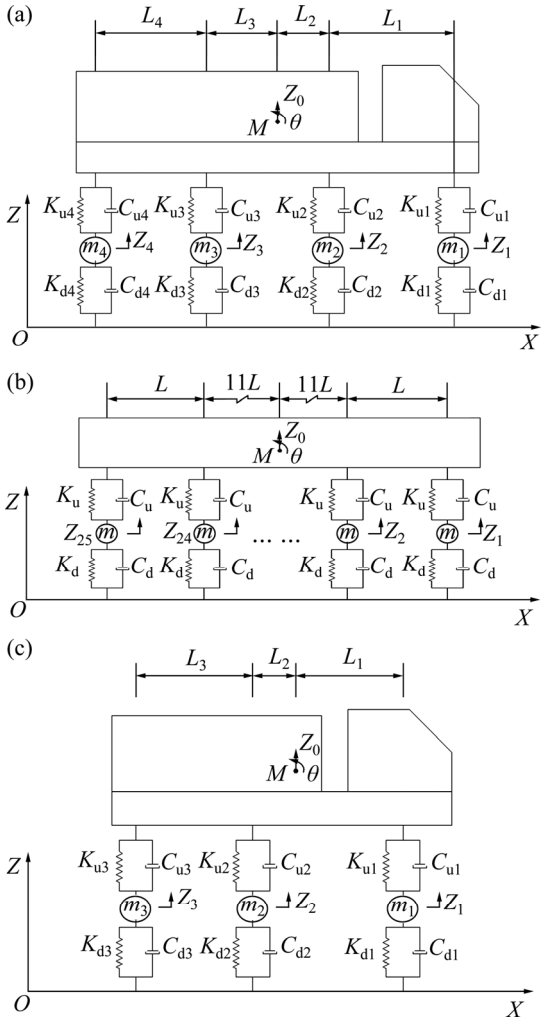

Fig. 2 Simplified vehicle model: (a) Tractor; (b) Flat-bed trailer; (c) Moped

By using the static equilibrium position of the vehicle as the reference point, the vertical displacement equation of endpoint i can be derived as

$$Z_{bi} = Z_0 + \theta x_i \tag{1}$$

where pitch angle θ is significantly small.

The use of generalized virtual work theory [6] provides the following:

$$\delta W_{\mathrm{v}} = M\ddot{Z}_0\delta Z_0 + \sum_{i=1}^{N} m_i\ddot{z}_i\delta Z_i + I_\theta\ddot{\theta}\delta\theta + \sum_{i=1}^{N} C_{ui}(\dot{Z}_{bi} - \dot{Z}_i)\delta(Z_{bi} - Z_i) + \sum_{i=1}^{N} K_{ui}(Z_{bi} - Z_i)\delta(Z_{bi} - Z_i) +$$

$$\sum_{i=1}^{N} C_{di}(\dot{Z}_i - \dot{Z}_{gi})\delta(Z_i - Z_{gi}) + \sum_{i=1}^{N} K_{di}(Z_i - Z_{gi})\delta(Z_i - Z_{gi}) = 0 \quad (2)$$

where δZ_0, δZ_i, and $\delta\theta$ are the generalized virtual displacements of the vehicle and are not zero; δZ_{gi} is the generalized virtual displacement of the bridge and is assumed to be equal to zero.

By incorporating Eqs. (1) and (2) and assuming that the corresponding coefficient terms of generalized virtual displacement are zero, the following equations are obtained.

$$M\ddot{Z}_0 + \sum_{i=1}^{N} C_{ui}(\dot{Z}_{bi} - \dot{Z}_i) + \sum_{i=1}^{N} K_{ui}(Z_{bi} - Z_i) = 0 \quad (3)$$

$$I_\theta\ddot{\theta} + \sum_{i=1}^{N} C_{ui}(\dot{Z}_{bi} - \dot{Z}_i)x_i + \sum_{i=1}^{N} K_{ui}(Z_{bi} - Z_i)x_i = 0 \quad (4)$$

$$m_i\ddot{Z}_i + C_{di}(\dot{Z}_i - \dot{Z}_{gi}) - C_{ui}(\dot{Z}_{bi} - \dot{Z}_i) + K_{di}(Z_i - Z_{gi}) - K_{ui}(Z_{bi} - Z_i) = 0 \quad (5)$$

Equations (3) to (5) denote the vertical motion equation of the body centroid, the pitching motion equation of the body, and the vertical motion equation of the wheels, respectively. x_i is the horizontal ordinate of the wheel.

The matrix form of the above formulas is expressed as

$$\boldsymbol{M}_v\ddot{\boldsymbol{u}}_v(t) + \boldsymbol{C}_v\dot{\boldsymbol{u}}_v(t) + \boldsymbol{K}_v\boldsymbol{u}_v(t) = \boldsymbol{F}_v(t) \quad (6)$$

where $\boldsymbol{M}_v$, $\boldsymbol{C}_v$, and $\boldsymbol{K}_v$ are the mass, damping, and stiffness matrices of the vehicle vibration subsystem, respectively; $\boldsymbol{F}_v(t)$ is the column vector of the excitation force; $\ddot{\boldsymbol{u}}_v(t)$, $\dot{\boldsymbol{u}}_v(t)$, and $\boldsymbol{u}_v(t)$ are the column vectors of the acceleration, velocity, and displacement of the vehicle vibration subsystem, respectively.

2.2 Continuous beam bridge model

The 2D finite element model of a continuous beam bridge was established, and the differential vibration equation in the form of a matrix is derived as

$$\boldsymbol{M}\ddot{\boldsymbol{u}}(t) + \boldsymbol{C}\dot{\boldsymbol{u}}(t) + \boldsymbol{K}\boldsymbol{u}(t) = \boldsymbol{F}(t) \quad (7)$$

where $\boldsymbol{M}$ is the mass matrix of the bridge, $\boldsymbol{C}$ is the damping matrix of the bridge, $\boldsymbol{K}$ is the stiffness matrix of the bridge, $\boldsymbol{F}(t)$ is the column vector of the vehicle–bridge interaction force, and $\ddot{\boldsymbol{u}}(t)$, $\dot{\boldsymbol{u}}(t)$, and $\boldsymbol{u}(t)$ are the nodal column vectors of acceleration, velocity, and displacement, respectively.

2.3 Displacement coordinate condition of vehicle–bridge system

Based on the assumption that the wheel is appressed on the deck when the vehicle is moving, the displacement coordinate equation and vehicle–bridge interaction force were derived as follows:

$$Z_{gi} = UZ(t, x_i) + Z_{ri} \quad (8)$$

$$P_i = W_i + C_{di}(\dot{Z}_i - \dot{Z}_{gi}) + K_{di}(Z_i - Z_{gi}) \quad (9)$$

where $UZ(t, x_i)$ is the deflection of the bridge node corresponding to wheel i, Z_{ri} is the surface roughness of the deck, and W_i is the sum of the self-weight and assigned static weight of wheel i. All values are negative when the direction is downward.

2.4 Numerical solution of vehicle–bridge coupled vibration

The second-order differential equations of the vehicle–bridge coupled vibration system contain variable coefficients, and the load entries are time-varying functions [7]. In most cases, direct integration method is utilized to solve these types of equations. The implicit Newmark-β integration method and finite element method were employed in this work to solve the differential equations of vehicle and bridge vibration. Displacement compatibility and interaction force equations were also adopted to consider vehicle–bridge coupling. The specific steps for solving the problem are shown below.

1) Establish the bridge model and determine the mass, stiffness, and damping matrix of the bridge subsystem.

2) Input the vehicle parameters and determine the mass, stiffness, and damping matrix of the vehicle subsystem.

3) Assume the initial state of the coupled vibration system.

4) Determine the interaction force of the bridge subsystem on the vehicle subsystem according to the displacement, velocity, and deck roughness of the bridge subsystem and establish the load vector shown as Eq. (6).

5) Utilize Newmark-β numerical iterative method to solve the differential equations of the vehicle subsystem and obtain its displacement, velocity, and acceleration vector.

6) Calculate the interaction force of the vehicle subsystem on the bridge subsystem and solve the differential equations of the latter.

7) Determine the convergence of the equilibrium iteration; if it satisfies the convergence criterion, then the iteration stops.

3 Measured deck roughness and power spectrum estimation

Uneven deck is one of the main causes of vehicle–bridge coupled vibration. Deck roughness is

divided into A to H according to power spectral density [8]. Power spectrum estimation and classification of measured deck roughness are necessary for the quantitative evaluation of the influence of deck roughness on the dynamic response of the vehicle–bridge system. Traditional power spectrum estimation method directly or indirectly applies Fourier transform to a limited number of sample data to obtain the power spectrum; this method has shortcomings, such as low resolution and poor variance performance [9]. The modern method of power spectrum estimation based on the AR model can provide an accurate estimate of the model parameters by solving linear equations and can obtain accurate power spectrum estimation.

Deck roughness is regarded as a Gaussian random process with zero mean, and roughness sequence $q(n)$ is assumed to meet the p order AR auto-regression model [10−11], namely,

$$q(n)=\sum_{k=1}^{p}a_k q(n-k)+w_{\mathrm{n}} \tag{10}$$

where w_{n} is a stationary white noise sequence with zero mean and variance σ_{w}^2; a_1, a_1, ⋯, a_p are real constants.

After the two sides of Eq. (10) are subjected to Z-transform, the transfer function and power spectral density function of the AR model can be obtained as shown in Eqs. (11) and (12), respectively.

$$H(Z)=\frac{1}{1+\sum_{k=1}^{p}a_k Z^{-k}} \tag{11}$$

$$S_{qq}(\omega)=\frac{\sigma_{\mathrm{w}}^2}{\left|1+\sum_{k=1}^{p}a_k \mathrm{e}^{-\mathrm{j}\omega k}\right|} \tag{12}$$

According to the nature of the autocorrelation function,

$$R_q(\tau)=\begin{cases}-\sum_{k=1}^{p}a_k R_q(\tau-k)+\sigma_{\mathrm{w}}^2, \tau=0\\ -\sum_{k=1}^{p}a_k R_q(\tau-k), \quad \tau\neq 0\end{cases} \tag{13}$$

where τ=1, 2, ⋯, p. According to the even function nature of the autocorrelation function, the Yule–Walker equations of the p order AR model are then obtained [12] as

$$\begin{bmatrix} R_q(0) & R_q(1) & R_q(2) & \cdots & R_q(p)\\ R_q(1) & R_q(0) & R_q(1) & \cdots & R_q(p-1)\\ R_q(2) & R_q(1) & R_q(0) & \cdots & R_q(p-2)\\ \vdots & \vdots & \vdots & & \vdots\\ R_q(p) & R_q(p-1) & R_q(p-2) & \cdots & R_q(0)\end{bmatrix}\cdot$$

$$\begin{bmatrix}1\\ a_1\\ a_2\\ \vdots\\ a_p\end{bmatrix}=\begin{bmatrix}\sigma_{\mathrm{w}}^2\\ 0\\ 0\\ \vdots\\ 0\end{bmatrix} \tag{14}$$

As shown in Eq. (12), the power spectrum of the AR model is determined by model parameters a_1, a_1, ⋯, a_p and white noise variance σ_{w}^2. After autocorrelation function $R_q(\tau)$ for sequence $q(n)$ is calculated with the measured deck roughness, the parameters of the AR model and white noise variance σ_{w}^2 can be calculated according to Eq. (14). The parameters and σ_{w}^2 should be incorporated into Eq. (12) to obtain the power spectral density of the AR model.

Figure 3 shows the measured deck roughness of Jiulong River Bridge at a sampling interval of 30 cm. Figure 4 shows the power spectrum of the measured deck roughness solved with the AR model. The measured sample is located in zone B [8].

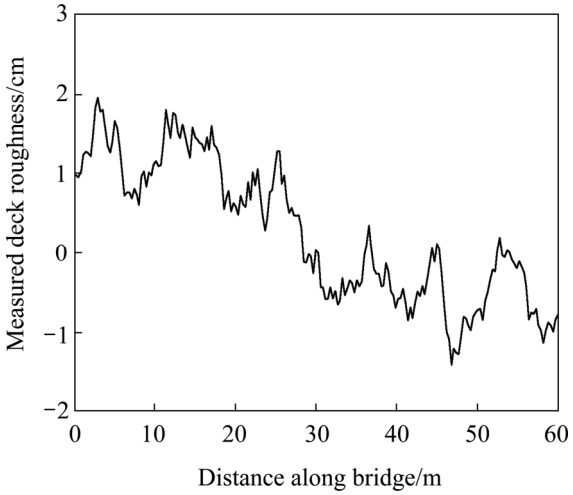

Fig. 3 Measured deck roughness

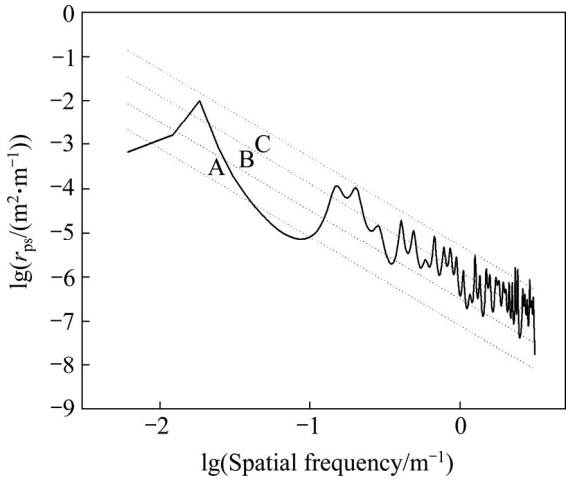

Fig. 4 Power spectrum of measured deck roughness (r_{ps} is power spectrum of deck roughness)

4 Dynamic response of continuous beam bridge under extra heavy vehicle

4.1 Calculation parameters

The dynamic response of the continuous beam bridge under the action of an extra heavy vehicle was calculated with the vehicle–bridge coupled vibration model. The initial values of vertical displacement, velocity, and acceleration were assumed to be zero. Newmark-β integration method was employed in the analysis. α was equal to 0.25, and β was equal to 0.5. The related parameters [13−15] are listed in Table 1.

Table 1 Vehicle parameters

Vehicle parameter	Tractor	Flat-bed trailer	Moped
Vehicle body mass/kg	35980	550350	32650
Vehicle body rotational inertia, I_θ/(kg·m^{-2})	59700	56825472	53700
Mass of a single wheel/kg	335	/	335
Stiffness of a single wheel, K_d/(MN·m^{-1})	2.4	/	2.4
Damping coefficient of a single wheel, C_d/(kN·s·m^{-1})	6	/	6
Suspension stiffness of a single wheel, K_u/(MN·m^{-1})	1.2	/	1.2
Suspension damping coefficient of a single wheel, C_u/(kN·s·m^{-1})	5	/	5
Mass of double wheels/kg	670	670	670
Stiffness of double wheels, K_d/(MN·m^{-1})	4.4	4.4	4.4
Damping coefficient of double wheels, C_d/(kN·s·m^{-1})	12	12	12
Suspension stiffness of double wheels, K_u/(MN·m^{-1})	2.4	2.4	2.4
Suspension damping coefficient of double wheels, C_u/(kN·s·m^{-1})	10	10	10
Distance parameter, L_1/m	2.10		3.70
Distance parameter, L_2/m	1.35		0.80
Distance parameter, L_3/m	1.35		2.10
Distance parameter, L_4/m	2.10		
Distance parameter, L/m		1.50	

The superstructure of Jiulong River Bridge is characterized by pre-stressed concrete continuous box girder. The span arrangement is 2 m×30 m. The cross section is shown in Fig. 5. The concrete strength grade is C50, with density ρ equal to 2500 kg/m^3 and elastic modulus E equal to 3.45×10^{10} Pa. The bending moment of inertia I is equal to 2.894, and the torsional moment of inertia J is equal to 7.681.

4.2 Calculation condition

Working condition 1 involves the solution of the vehicle–bridge coupled vibration model with smooth deck. Working condition 2 involves the solution of the vehicle–bridge coupled vibration model with measured deck roughness. Working condition 3 involves validation by transient dynamic method. Transient dynamic method was utilized to analyze the dynamic response of the bridge under vehicle load and verify the established vehicle–bridge coupled vibration model. Vehicle loads were simplified as constant force on the bridge. The wheel force on the bridge node was regarded as a type of shock load that disappears after instantaneous action; it can be approximately simulated as triangular load as shown in Fig. 6.

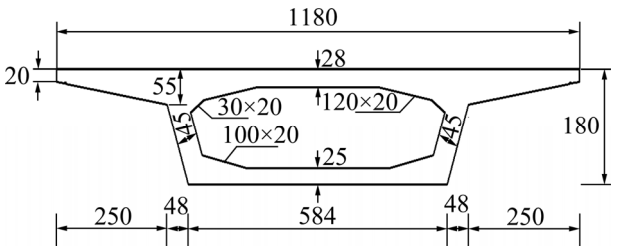

Fig. 5 Cross-section of box girder (Unit: cm)

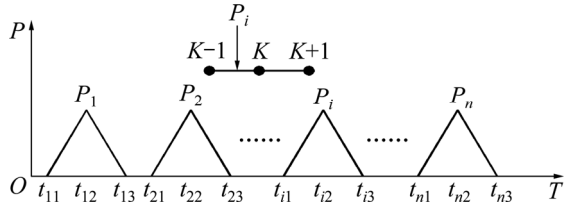

Fig. 6 Simulation of wheel load (Note: Time difference t_{ij} is determined by vehicle speed and node spacing; P_i denotes single wheel load; t_{i1}, t_{i2}, and t_{i3} denote time when wheel i arrives at nodes K−1, K, and K+1; $L_{K-1,K}$ denotes the length of element with node K−1 and K; $L_{K,K+1}$ denotes the length of element with node K and K+1; and V denotes vehicle velocity; $t_{i2}-t_{i1}=\frac{L_{K-1,\ K}}{V}$; $t_{i3}-t_{i2}=\frac{L_{K,\ K+1}}{V}$.)

4.3 Vibration characteristics of vehicle

The natural vibration characteristics of the tractor, flat-bed trailer, and moped were analyzed according to the established vehicle model. The first two orders of natural vibration frequency are listed in Table 2.

Table 2 Frequency and vibration response of vehicle

Vehicle	Order	Frequency/Hz	Modal description
Tractor	1	2.415	Translation
	2	5.142	Pitching
Flat-bed trailer	1	2.302	Translation
	2	2.449	Pitching
Moped	1	2.232	Translation
	2	4.971	Pitching

4.4 Dynamic response of continuous beam under an extra heavy vehicle

An extra heavy vehicle for over-sized transport is usually required to drive through a bridge at low speed (<10 km/h) along a delineated lane [16]. Figure 7 shows the dynamic response of the continuous beam bridge when the extra heavy vehicle (shown in Fig. 2) passes through at a speed of 5 km/h. Figures 7 and 8 show that the results of working conditions 1 and 3 exhibit almost the same trend. The absolute value of the peak in condition 1 is greater than that in condition 3. This result indicates that the dynamic response of the continuous beam bridge increased in consideration of vehicle–bridge coupled vibration and thus verifies the established model. When the measured deck roughness (shown in Fig. 3) was considered, the vibration of the continuous beam under the action of the extra heavy vehicle intensified. The dynamic response (maximum deflection, maximum bending moment, and maximum shear) of the sections in the left span became smaller than those in conditions 1 and 3. However, the dynamic response of the sections in the right span became greater than those in conditions 1 and 3.

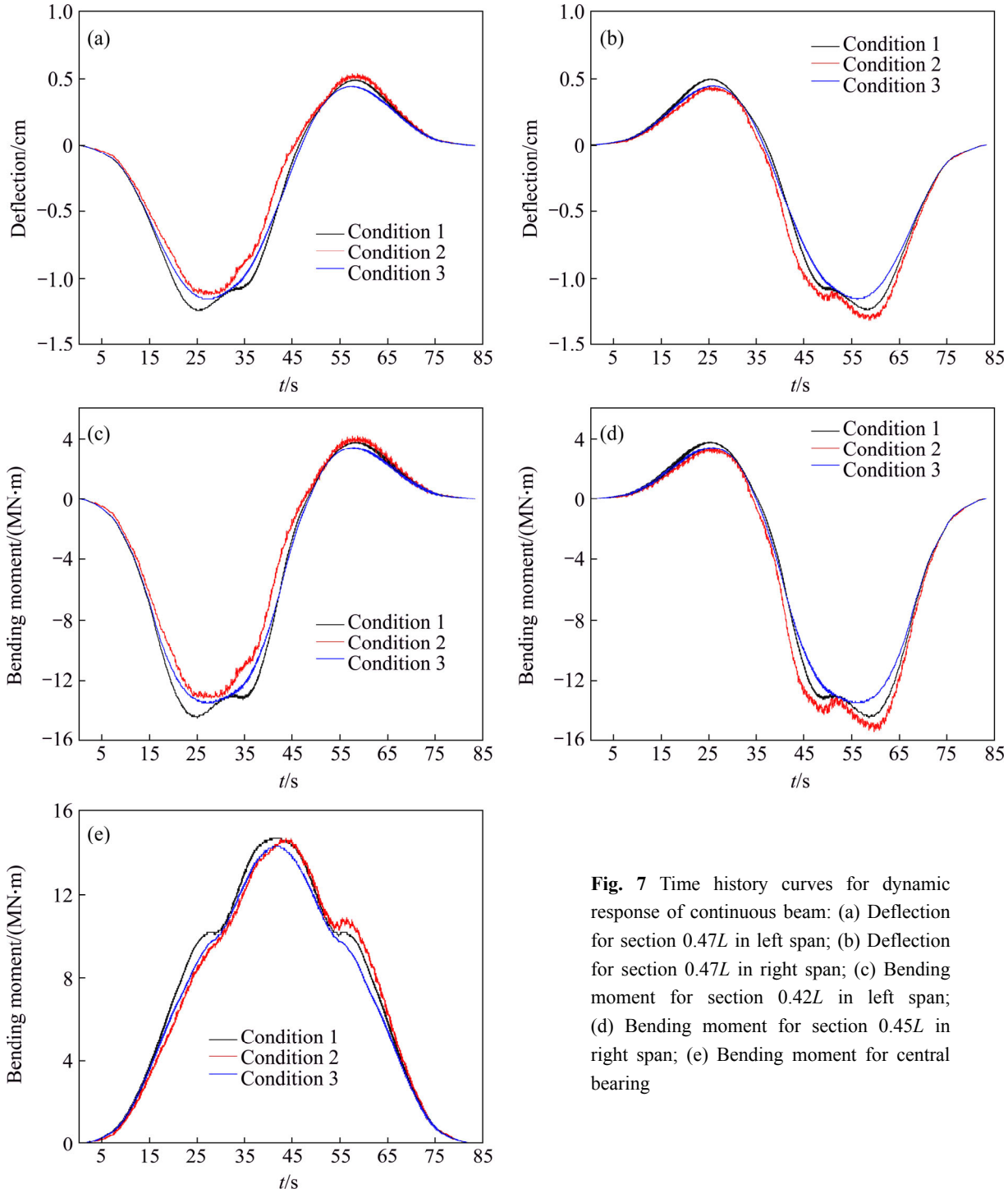

Fig. 7 Time history curves for dynamic response of continuous beam: (a) Deflection for section 0.47*L* in left span; (b) Deflection for section 0.47*L* in right span; (c) Bending moment for section 0.42*L* in left span; (d) Bending moment for section 0.45*L* in right span; (e) Bending moment for central bearing

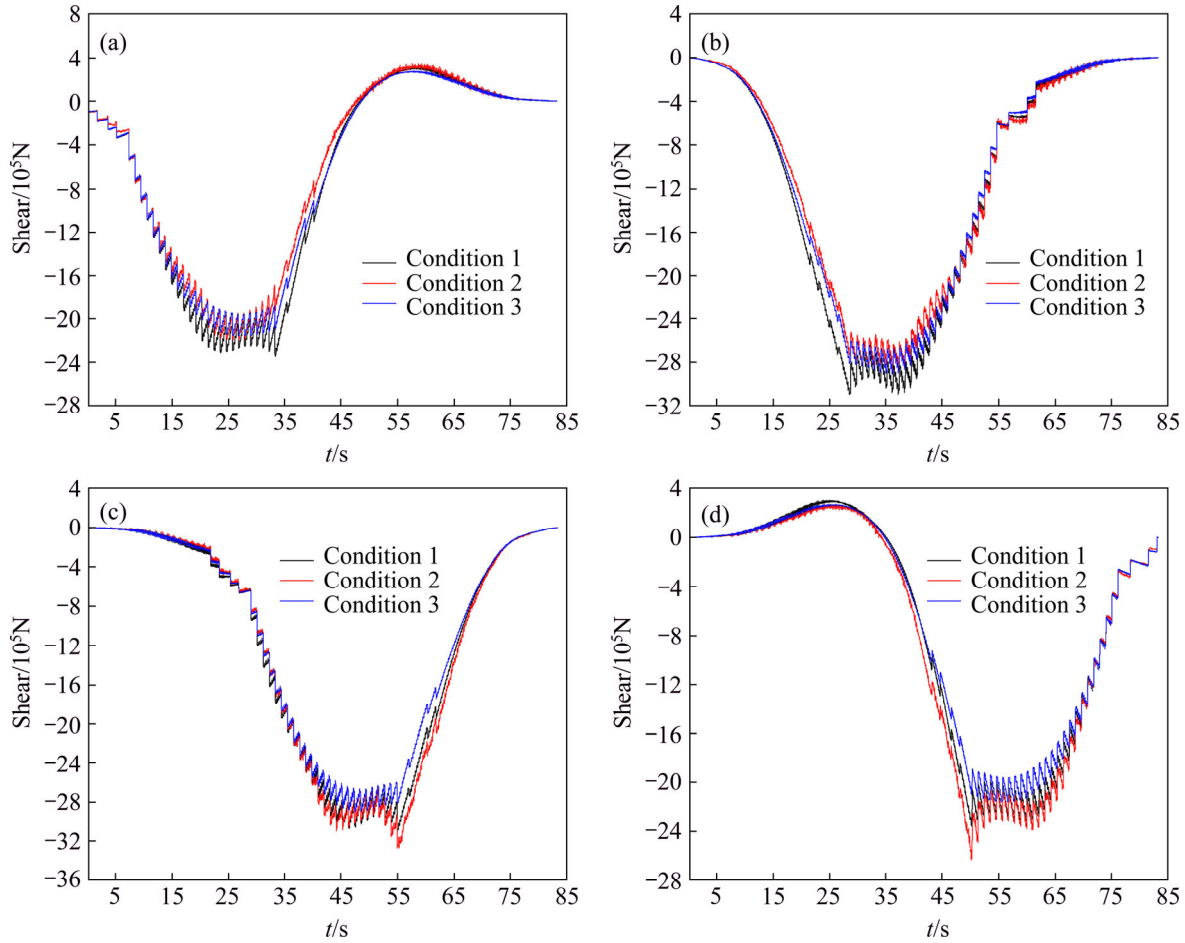

Fig. 8 Time history curves for dynamic response of continuous beam: (a) Shear for left bearing; (b) Shear for left section of central bearing; (c) Shear for right section of central bearing; (d) Shear for right bearing

4.5 Impact effect of continuous beam under extra heavy vehicle

Influenced by many complex factors, the dynamic effects of moving vehicles on bridges are greater than the static effects in most cases. The effect of vehicles is defined as the impact coefficient as shown below.

$$1+\mu=\frac{A_{\mathrm{dyn}}}{A_{\mathrm{st}}} \tag{15}$$

where A_{dyn} is the peak of dynamic deflection for the bridge's mid-span section when the vehicle passes through it; A_{st} denotes the corresponding static value. Currently, only the fundamental frequency of a structure is considered in the calculation of the bridge impact coefficient in Chinese specifications. However, deck roughness, vehicle speed, connection stiffness, and damping between the various parts of the vehicle are also closely related to the impact coefficient.

The impact coefficient for the control section of the continuous beam was calculated according to Eq. (15) and is listed in Table 3 when the extra heavy vehicle passes through the bridge at a low speed of 5 km/h. Although the calculated values are less than those indicated in literature [17], the impact effect induced by the vehicle driving at low speed should not be neglected. This condition means that the impact effect of vehicle load must be considered in bridge safety assessment for over-sized transport with low speed.

According to the transformational relation among the different levels of deck roughness, the samples of levels A, C, and D can be obtained by multiplying the measured deck roughnesses by 0.5, 2.0, and 4.0. The impact coefficient for the control section of the continuous beam with different levels of deck roughness under different vehicle speeds is shown in Fig. 9. When the vehicle speed is low, the impact coefficient is not necessarily small. On the contrary, the impact coefficient for vehicle speed of 5 km/h is greater than that for 10 km/h, a result that is consistent with research results in Ref. [18]. Deck roughness has a significant influence on the impact coefficient, which increases with the increase in deck roughness level. Although deck roughness in China can basically be ranked from level A to level C and level D deck roughness is rare, special attention should still be provided to level D because of the significant increase in the impact coefficient.

Table 3 Impact coefficient of continuous beam under extra heavy vehicle

Impact coefficient, μ	Deflection for section 0.47L in right span	Bending moment for section 0.45L in right span	Bending moment for central bearing	Shear for right section of central bearing	Shear for right bearing
Calculated value	0.146	0.140	0.037	0.137	0.193
Standard value	0.212	0.212	0.291	0.212	0.212

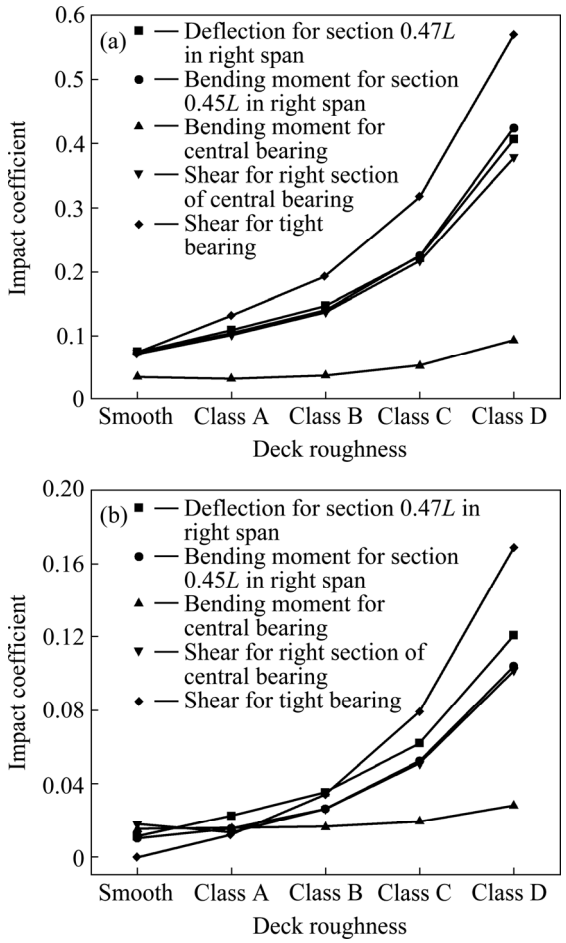

Fig. 9 Impact coefficient of continuous beam bridge: (a) Vehicle speed of 5 km/h; (b) Vehicle speed of 10 km/h

Given that no specific law exists between the impact coefficient and vehicle speed and that deck roughness plays an important role, unduly limiting vehicle speed is unnecessary. Deck treatment is an effective method of decreasing the vehicle impact effect. Table 4 shows the recommended values of the impact coefficient for the continuous beam with different levels of deck roughness and provides reference for bridge bearing capacity assessment under the action of an extra heavy vehicle. In this work, although the impact coefficient for negative bending moment is small because of the distribution characteristic of deck roughness, a large impact coefficient can still be generated with other deck roughness samples with different distribution characteristics. Considering that the impact coefficient for negative bending moment in Ref. [17] is greater than that for positive bending moment, the recommended impact coefficient for negative bending moment in Table 4 is equal to that for positive bending moment.

5 Reliability assessment of continuous beam based on Matlab optimization toolbox

5.1 Establishment of optimization model for solving reliability index β

Structural reliability refers to the probability of accomplishing a predetermined function within the prescribed time and conditions. Assuming that $\boldsymbol{X}=(X_1, X_2, \cdots, X_n)^{\mathrm{T}}$ denotes the n random variables that affect the structural function and that the probability distribution function of the variable is $F_i(X_i)(i=1, 2, \cdots, n)$, the function can then be expressed by n random variables as follows:

$$Z_X = g(X) = g(X_1, X_2, \cdots, X_n) \tag{16}$$

When $Z\geq 0$, the structure is in a reliable state; when $Z<0$, the structure is in a state of failure. Assuming that failure probability $P_f=\Phi(-\beta)$ and β is the reliability index, then a one-to-one relationship exists between P_f and β.

Mapping transformation [19] yields

$$F_i(X_i) = \Phi(Y_i) \ \ (i = 1,2,\cdots n) \tag{17}$$

Thus,

$$X_i = F_i^{-1}[\Phi(Y_i)] \tag{18}$$

where $F_i^{-1}[\cdot]$ denotes the inverse function of distribution function $F_i(\cdot)$; $\Phi(\cdot)$ denotes the standard normal distribution function; Y_i denotes the independent standard normal random variable.

Incorporating Eq. (18) into Eq. (16) yields

$$\begin{aligned} Z_Y &= g(F_1^{-1}[\Phi(Y_1)], F_2^{-1}[\Phi(Y_2)], \cdots, F_n^{-1}[\Phi(Y_n)]) \\ &= G(Y_1, Y_2, \cdots, Y_n) \end{aligned} \tag{19}$$

According to the geometric meaning of reliability index β in standard normal space,

$$\begin{cases} \min \ \beta = \sqrt{Y_1^2 + Y_2^2 + \cdots + Y_n^2} \\ \text{s.t.} \quad G(Y_1, Y_2, \cdots, Y_n) = 0 \end{cases} \tag{20}$$

Obviously, objective function β is a convex function. If $G(Y_1, Y_2, \cdots, Y_n)=0$ is also a convex function, then the model (Eq. (20)) is a convex programming problem. According to the optimization principle, any local minimum point of the model is the global minimum point of objective function β in a non-empty feasible set.

Table 4 Recommended value of impact coefficient for different levels of road surface roughness

Surface	Positive bending moment and shear		Recommended value	Negative bending moment		Recommended value
	5 km/h	10 km/h		5 km/h	10 km/h	
Smooth road surface	0.071–0.074	0.000–0.017	0.10	0.035	0.015	0.10
Level A road surface	0.101–0.131	0.012–0.022	0.15	0.032	0.015	0.15
Level B road surface	0.137–0.193	0.026–0.035	0.20	0.037	0.016	0.20
Level C road surface	0.217–0.317	0.051–0.079	0.35	0.052	0.019	0.35
Level D road surface	0.378–0.570	0.102–0.169	0.60	0.093	0.028	0.60

Therefore, this method requires that the function $G(Y_1, Y_2, \cdots, Y_n)=0$ is convex in standard normal space; otherwise, the applicability of the solution cannot be guaranteed.

5.2 Solving steps for reliability index β [20]

Step 1: Determine random variable X_i and its probability distribution function $F_i(X_i)$ and ultimate state function $Z_X=g(X_1, X_2,\cdots, X_n)=0$.

Step 2: Implement mapping transformation according to Eq. (17) and obtain independent standard normal random variable Y_i.

Step 3: Substitute Y_i into Eq. (20) and obtain the optimization model for solving reliability index β.

Step 4: Utilize command fmincon from the Matlab optimization toolbox and solve model (Eq. (20)) to obtain reliability index β.

5.3 Failure criteria for sections of bridge structure

According to Ref. [21], the failure criterion of bending resistance for each section is

$$R < \gamma_0(\gamma_G S_{Gk} + \gamma_Q S_{Qk}) \tag{21}$$

where R is the ultimate bearing capacity for section bending resistance; γ_0 denotes the importance factor of the structure (1.0 in this work); S_{Gk} denotes the standard value of self-weight effect and second phase dead load effect; γ_G=1.2 is the partial coefficient; S_{Qk} denotes the standard value of the extra heavy vehicle effect; γ_Q=1.1 is the partial coefficient.

5.4 Probability model for structure resistance and load effect

According to related regulations mentioned in Ref. [22] and the actual situation of Jiulong River Bridge, the probability distribution for section resistance was obtained as listed in Table 5. The probability distribution of load effect was likewise obtained as listed in Table 6.

5.5 Reliability assessment of continuous beam under action of extra heavy vehicle

In theory, the minimum reliability index of a bridge structure under the action of an extra heavy vehicle should be determined through optimization method according to the importance of the structure and equipment, failure consequences, nature of the destruction, economic index, and so on. However, establishing a quantitative analysis method is extremely difficult. For second-level highway bridges, it has been specified that the target reliability index is 4.2 for ductile failure and 4.7 for brittle failure [22], which has an adjustment range of not more than ±0.25 when well founded. Therefore, the minimum reliability index of a bridge under the action of an extra heavy vehicle is 3.95 for ductile failure and 4.45 for brittle failure.

Table 5 Probability distribution of section resistance

Resistance pattern	Distribution pattern	Mean value/eigenvalue	Variance coefficient
Bending resistance	Log normal distribution	1.2262	2.1798
Shear resistance	Log normal distribution	0.1414	0.2230

Table 6 Probability distribution of load effect

Load pattern	Distribution pattern	Mean value/eigenvalue	Variance coefficient
Self weight	Gaussian distribution	1.0148	0.0431
Extra heavy vehicle	Gaussian distribution	1.00	0.05

Table 7 shows the failure probability of the control sections with different levels of deck roughness obtained with the Matlab optimization toolbox. Figure 10 shows the corresponding reliability index β. As can be seen in the figure, the reliability of the continuous beam decreases as the deck roughness level increases. When the deck roughness reaches level C, the bending resistance reliability index for the 0.45L section of the right span is 3.88, which is lower than the minimum reliability index of 3.95. When the deck roughness reaches level D, the shear resistance reliability index for the right bearing section is 3.06, which is lower than the minimum reliability index of 4.45. For the continuous beam bridge in this study, the deck roughness is in level B and the reliability indices of the control sections are all greater than the minimum reliability index. Thus, no reinforcement measures are required for the over-sized transport.

Table 7 Failure probability for control sections

Road surface level	Bending moment for section 0.45L in right span	Bending moment for central bearing	Shear for right section of central bearing	Shear for right bearing
Smooth	1.75×10^{-7}	6.35×10^{-8}	1.77×10^{-18}	3.07×10^{-18}
Level A	6.24×10^{-7}	5.40×10^{-8}	2.49×10^{-17}	1.55×10^{-15}
Level B	2.79×10^{-6}	7.03×10^{-8}	4.69×10^{-16}	5.37×10^{-13}
Level C	5.25×10^{-5}	1.42×10^{-7}	2.09×10^{-13}	5.45×10^{-9}
Level D	1.03×10^{-2}	8.58×10^{-7}	5.37×10^{-9}	1.10×10^{-3}

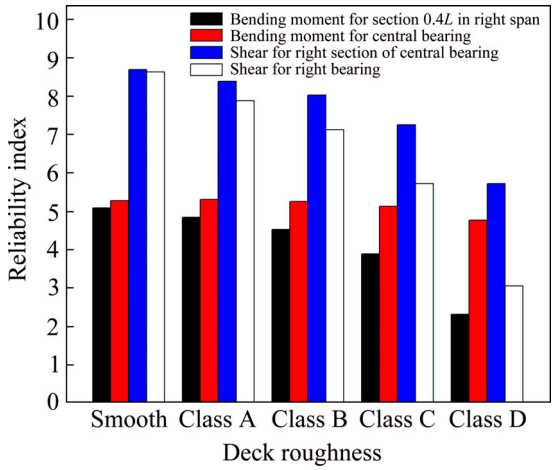

Fig. 10 Reliability index β of control sections

6 Conclusions

1) The established model can accurately simulate the dynamic characteristics of the actual vehicle, such as ups and downs and pitch. With regard to the simulation of deck roughness, the model can also accurately analyze the dynamic response of the bridge under the action of an extra heavy vehicle.

2) Power spectrum estimation method based on the AR model can help to quantitatively analyze the influence of measured deck roughness on the dynamic response of the bridge with considerable accuracy.

3) When the extra heavy vehicle passes the continuous beam bridge with B-grade deck roughness at a speed of 5 km/h, the maximum impact coefficient reaches 0.193, which should not be disregarded in bridge safety assessment.

4) No specific law exists between the impact coefficient and vehicle speed. However, the influence of deck roughness is significant. Unduly limiting the vehicle speed is unnecessary, and deck roughness repairing is an effective means to reduce the impact effect.

5) Deck roughness has a significant influence on the reliability index, which decreases as the deck roughness level increases. For the continuous beam bridge, the reliability indices of the control sections are all greater than the minimum reliability index; thus, no reinforcement measures are required for over-sized transport.

References

[1] XING Wen-bang. Rapid assessment method research on bridge during oversize transport [J]. Journal of China & Foreign Highway, 2011, 31(3): 217−220. (in Chinese)

[2] LIU Yao, YE Gui-ru, ZHANG Zhi-cheng. Method “bridge on the bridge” used in the massive product transportation [J]. Journal of Wuhan University of Technology: Transportation Science & Engineering, 2008, 32(1): 176−179. (in Chinese)

[3] QIAN Hong, MENG Yun, ZHANG Hui-li. A special application of temporary steel bridge in heavy-cargo transportation [J]. Journal of Chongqing Jiaotong University, 2005, 24(5): 10−13. (in Chinese)

[4] SHI Ying, SONG Yi-fan, SUN Hui. Dynamic analysis method of vehicle-bridge coupling for complicated bridges based on ANSYS [J]. Journal of Tianjin University, 2010, 43(6): 537−543. (in Chinese)

[5] LI Xiao-zhen, ZHANG Li-ming, ZHANG Jie. State-of-the-art review and trend of studies on coupling vibration for vehicle and highway bridge system [J]. Engineering Mechanics, 2008, 25(3): 230−240.

[6] ZENG Qing-yuan. The principle of total potential energy with stationary value in elastic system dynamics [J]. Journal of Huazhong University of Science and Technology, 2000, 28(1): 1−3. (in Chinese)

[7] GUO Wen-hua, CHEN Dai-hai, LI Zheng. Influence of secondary dead load on vehicle-bridge coupling vibration of long-span cable-stayed bridges [J]. Journal of Central South University: Science and Technology. 2011, 42(8): 2423−2429. (in Chinese)

[8] GB7031—1986 Vehicle vibration-describing method for road surface irregularity [S]. (in Chinese)

[9] Feisi Science and Technology Research Center. MATLAB7 aided signal processing technology and application [M]. Bejing: Electronics Industry Press, 2005. (in Chinese)

[10] ZOU Kun, YUAN Jun-quan, GONG Xiang-yi. MATLAB6.X signal processing [M]. Beijing: Tsinghua University Press, 2002. (in Chinese)

[11] YANG Shu-zi, WU Ya, XUAN Jian-ping. Time series analysis in engineering application [M]. Wuhan: Huazhong University of Science and Technology Press, 2007. (in Chinese)

[12] HU Guang-shu. Digital signal processing: Theory, algorithm and realization [M]. Beijing: Tsinghua University Press, 1996. (in Chinese)

[13] ZHONG Yang, ZHOU Fu-lin, ZHANG Yong-shan. Dynamic response to a plate on elastic foundation under moving load with varying velocity [J]. Journal of Vibration and Shock, 2008, 27(1): 61−64.

[14] HAN Wan-shui, MA Lin, YUAN Su-jing, ZHAO Sheng-min. Analysis of the effect of inconsistent stimulus of surface roughness on vehicle-bridge coupling vibrations [J]. China Civil Engineering Journal, 2011, 44(10): 81−90. (in Chinese)

[15] ZHOU Xin-ping, SONG Yi-fan, HE Shuan-hai. Numerical analysis for coupled vibration of vehicle-bridgeon highway curved bridge [J]. Journal of Chang’an University: Natural Science Edition, 2009, 29(6): 41−46. (in Chinese)

[16] JTG/T J21—2011. Specifications for inspection and evaluation of the bearing ability of highway bridges [S]. (in Chinese)

[17] JTG D60—2004. General code for design of highway bridges and culverts. Beijing: The People’s Communications Publishing House,

2004. (in Chinese)

[18] TAN Guo-jin, LIU Han-bing, CHENG Yong-chun. Analysis of impact of vehicle to simply supported beam [J]. Journal of Jilin University: Engineering and Technology Edition, 2011, 41(1): 62−67. (in Chinese)

[19] GUI Jing-song, KANG Hai-gui. The structural reliability calculation base on Matlab [J]. Sichuan Building Science, 2004, 30(2): 18−20. (in Chinese)

[20] LI Zhi-hua, HANG Guang-hai, KANG Hai-gui. Research for reliability of engineering structures based on Matlab's optimization tool box [J]. Sichuan Building Science, 2005, 31(3): 1−4. (in Chinese)

[21] YAN Lei, LU Ying-zhao, HE Shuan-hai. Reliability of existing concrete bridge [J]. Journal of Chang'an University: Natural Science Edition, 2009, 29(1): 50−53. (in Chinese)

[22] GB/T 50283—1999. Unified standard for reliability design of highway engineering structures [S]. (in Chinese)

(Edited by DENG Lü-xiang)